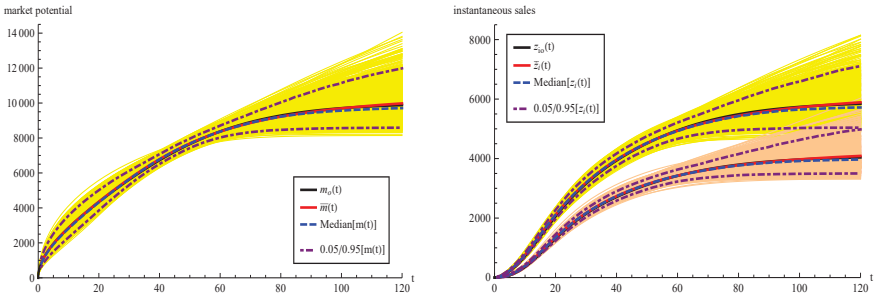

FIG A5.11. *Case* $_{\omega}\sigma_i = 0.20$. *Left side:* $\hat{m}_k(t)$ *(yellow trajectories), true* $m_0(t)$, $\overline{m}(t) = \frac{1}{1000}\sum_{k=1}^{1000}\hat{m}_k(t)$, *median trajectory, and quantile trajectories (0.05 and 0.95). Right side:* $\hat{z}_{ik}(t)$ *(yellow and orange trajectories), true* $z_{i0}(t)$, $\overline{z}_i(t) = \frac{1}{1000}\sum_{k=1}^{1000}\hat{z}_{ik}(t)$, *median trajectory, and quantile trajectories (0.05 and 0.95).*

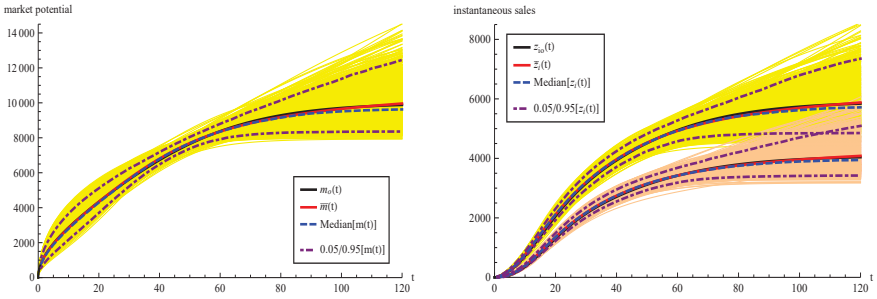

FIG A5.12. *Case* $_{\omega}\sigma_i = 0.25$. *Left side:* $\hat{m}_k(t)$ *(yellow trajectories), true* $m_0(t)$, $\overline{m}(t) = \frac{1}{1000}\sum_{k=1}^{1000}\hat{m}_k(t)$, *median trajectory, and quantile trajectories (0.05 and 0.95). Right side:* $\hat{z}_{ik}(t)$ *(yellow and orange trajectories), true* $z_{i0}(t)$, $\overline{z}_i(t) = \frac{1}{1000}\sum_{k=1}^{1000}\hat{z}_{ik}(t)$, *median trajectory, and quantile trajectories (0.05 and 0.95).*

of the true $z_i(t)$ functions, the estimated mean trajectories $\hat{z}_{ik}(t)$, $\overline{z}_i(t) = \frac{1}{1000}\sum_{k=1}^{1000}\hat{z}_{ik}(t)$, the median trajectory, and the quantile trajectories (0.05 and 0.95). For ${}_{\omega}\sigma_i$ values up to 0.15, all the estimated trajectories are very close to the true one even for long-term forecasting ($t \leq 75$). For ${}_{\omega}\sigma_i = 0.20$, uncertainty is moderate for medium-term forecasting ($t \leq 60$), while fluctuations around the true trajectories make forecasts less reliable for ${}_{\omega}\sigma_i$ exceeding 0.20. It is notable, however, that the average trajectories, $\overline{m}(t)$ and $\overline{z}_i(t)$, are essentially coincident with the respective true functions, $m_0(t)$ and $z_{0i}(t)$.

A5.2. *Alternative market potential structures.* The simulations shed light on one further key point. The described results were obtained with a "correctly specified" $m(t)$ function, function (2.4). To determine whether the proposed model could also adequately describe data generated with a more complex dynamic than (2.4)—and what implications such a misspecification in the market potential dynamics would have for evolutionary parameters p_1, q_1, p_2, q_2, and δ—we examined alternative $m(t)$ functions for data generation. The structure (2.4) represents a communication network's size growing according to a simple Bass model. Pertaining sensible assumptions about knowledge spread may lead to heterogeneous behavior of involved agents. In the literature, this effect has been modeled through more complex diffusion of innovation models either with a continuous approach (see, e.g., Bemmaor, 1994; Bemmaor and Lee, 2002) or with a discrete approach (see, e.g., Karmeshu and Goswami, 2001). The former leads to the alternative specification

$$m(t) = K\frac{[1-e^{-(p_c+q_c)t}]^{\beta}}{[1+\frac{q_c}{p_c}e^{-(p_c+q_c)t}]^{\alpha}}, \quad K, p_c, q_c, \alpha, \beta > 0, \quad t > 0, \tag{A5.8}$$

while the latter gives rise to a two-wave model,

$$m(t) = K_1\frac{1-e^{-(p_{1c}+q_{1c})t}}{1+\frac{q_{1c}}{p_{1c}}e^{-(p_{1c}+q_{1c})t}} + K_2\frac{1-e^{-(p_{2c}+q_{2c})(t-t_c)}}{1+\frac{q_{2c}}{p_{2c}}e^{-(p_{2c}+q_{2c})(t-t_c)}}I_{t\geq tc}, \tag{A5.9}$$

where $K_i, p_{ic}, q_{ic}, t_c > 0$, $t > 0$.

Specifically, we present the results obtained for

- a Bemmaor model (A5.8) with $\alpha = 0.25$ and $\beta = 0.5$ (BE(0.25,0.5)),
- a Bemmaor model (A5.8) with $\alpha = 1$ and $\beta = 0.5$ (BE(1,0.5)),
- a two–wave model (A5.9) with changepoint in $tc_c = 20$ (TW(20)).

Notice that function (2.4) can be represented as BE(0.5,0.5), as it is obviously a special case of (A5.8).

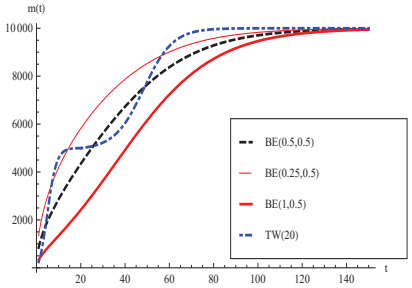

FIG A5.13. *Alternative $m(t)$ dynamics used in simulations: a Bemmaor model (A5.8) with $\alpha = 0.25$ and $\beta = 0.5$ (BE(0.25,0.5)), a Bemmaor model (A5.8) with $\alpha = 1$ and $\beta = 0.5$ (BE(1,0.5)) a two-wave model (A5.9) with changepoint in $tc_c = 20$ (TW(20)). The $m(t)$ function used throughout the paper, (2.4), is also plotted and denoted by BE(0.5,0.5).*

TABLE A5.6
MISE for the market potential function, $m(t)$, with alternative specifications.

		$T = 50$	$T = 60$	$T = 70$	$T = 88$	$T = 114$
BE(0.5,0.5)	${}_{\omega}\sigma_i = 0.05$	7.9842*10^5	8.4136*10^5	9.5680*10^5	1.8808*10^6	6.7524*10^6
	${}_{\omega}\sigma_i = 0.10$	1.0264*10^6	1.1166*10^6	1.3408*10^6	2.8253*10^6	9.2680*10^6
	${}_{\omega}\sigma_i = 0.15$	1.6529*10^6	1.8306*10^6	2.2428*10^6	4.7968*10^6	1.5172*10^7
BE(0.25,0.5)	${}_{\omega}\sigma_i = 0.05$	1.0649*10^6	1.1039*10^6	1.2103*10^6	2.1663*10^6	8.4540*10^6
	${}_{\omega}\sigma_i = 0.10$	2.0646*10^6	2.1692*10^6	2.3584*10^6	3.4547*10^6	9.2892*10^6
	${}_{\omega}\sigma_i = 0.15$	3.9747*10^6	4.1821*10^6	4.5231*10^6	6.1057*10^6	1.3061*10^7
BE(1,0.5)	${}_{\omega}\sigma_i = 0.05$	1.4031*10^6	1.4457*10^6	1.6207*10^6	4.1432*10^6	1.7707*10^7
	${}_{\omega}\sigma_i = 0.10$	2.7012*10^6	2.8158*10^6	3.4295*10^6	1.0847*10^7	6.0820*10^7
	${}_{\omega}\sigma_i = 0.15$	3.2451*10^6	3.4712*10^6	4.5917*10^6	1.7575*10^7	1.1643*10^8
TW(20)	${}_{\omega}\sigma_i = 0.05$	5.2213*10^7	5.4527*10^7	5.5356*10^7	1.3536*10^8	1.2534*10^9
	${}_{\omega}\sigma_i = 0.10$	5.2346*10^7	5.4871*10^7	5.5799*10^7	1.3644*10^8	1.2625*10^9
	${}_{\omega}\sigma_i = 0.15$	5.3285*10^7	5.5762*10^7	5.6861*10^7	1.4162*10^8	1.2932*10^9

Figure A5.13 shows the plot of these alternative dynamic structures in comparison with the original function used in previously described simulations. For comparative purposes, we show here the results obtained with the three alternatives for the less extreme values of ${}_{\omega}\sigma_i$ (namely 0.05, 0.10, and 0.15).

Table A5.6 shows the MISE values. When a BE(0.25,0.5) structure is used to simulate the data, the MISE values are remarkably close to the BE(0.5,0.5) case, and for higher T values, the MISE is even smaller. The BE(1,0.5) model makes a somewhat greater impact on the MISE. Figures A5.14–A5.19 show the true and estimated trajectories for the dynamic market potential and the fitted response, when $m(t)$ is simulated through a Bemmaor process. The fluctuations are higher, especially when BE(1.0.5) is

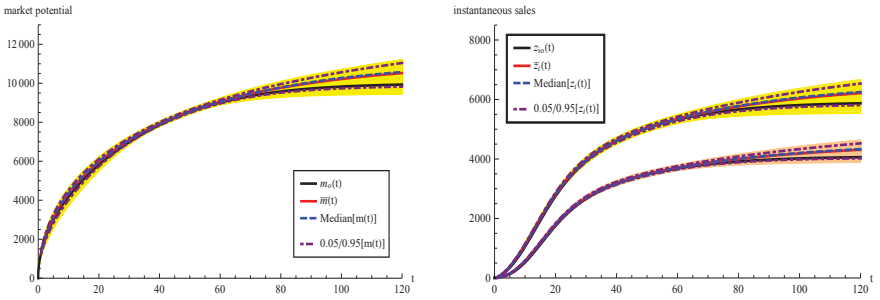

FIG A5.14. *Case BE(0.25,0.5),* $_{\omega}\sigma_i = 0.05$. *Left side:* $\hat{m}_k(t)$ *(yellow trajectories), true* $m_0(t)$, $\overline{m}(t) = \frac{1}{1000}\sum_{k=1}^{1000}\hat{m}_k(t)$, *median trajectory, and quantile trajectories (0.05 and 0.95). Right side:* $\hat{z}_{ik}(t)$ *(yellow and orange trajectories), true* $z_{i0}(t)$, $\overline{z}_i(t) = \frac{1}{1000}\sum_{k=1}^{1000}\hat{z}_{ik}(t)$, *median trajectory, and quantile trajectories (0.05 and 0.95).*

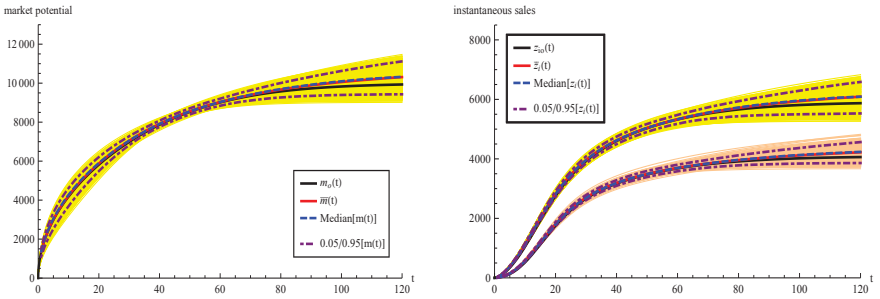

FIG A5.15. *Case BE(0.25,0.5),* $_{\omega}\sigma_i = 0.10$. *Left side:* $\hat{m}_k(t)$ *(yellow trajectories), true* $m_0(t)$, $\overline{m}(t) = \frac{1}{1000}\sum_{k=1}^{1000}\hat{m}_k(t)$, *median trajectory, and quantile trajectories (0.05 and 0.95). Right side:* $\hat{z}_{ik}(t)$ *(yellow and orange trajectories), true* $z_{i0}(t)$, $\overline{z}_i(t) = \frac{1}{1000}\sum_{k=1}^{1000}\hat{z}_{ik}(t)$, *median trajectory, and quantile trajectories (0.05 and 0.95).*

used and $t \geq 80$. For higher t values, the average trajectories are not fully coincident with the true ones. This is unsurprising, as the estimation procedure makes use of data from $t = 1$ to $t = 50$; a good approximation of a Bemmaor structure through a Bass model in the range $[1, 50]$ may not be equally good in a different range.

Finally, the two-wave model (TW(20)) produces MISE values that are ten times greater than the BE(0.5,0.5) model. Figures A5.20–A5.22 show the true and estimated trajectories for dynamic market potential and the fitted response when $m(t)$ is simulated through a two-wave process. In this case, $m(t)$ cannot be adequately described even for smaller t values, but the fluctuations around $z_{0i}(t)$ are extremely small for $t \leq 60$.

Table A5.7 shows the MSE for the estimates of $(p_1, q_1, p_2, q_2, \delta)$ with the